Max-Planck-Institut für Plasmaphysik
Garching bei München

Understanding and improving the neutral beam injector conditioning problem

Edward C.A. Morris

IPP 4/250 **September 1991**

Die nachstehende Arbeit wurde im Rahmen des Vertrages zwischen dem Max-Planck-Institut für Plasmaphysik und der Europäischen Atomgemeinschaft über die Zusammenarbeit auf dem Gebiete der Plasmaphysik durchgeführt

Understanding and improving the neutral beam injector conditioning problem

E.C.A. Morris

Max-Planck-Institut für Plasmaphysik
Euratom-Association, D 8046 Garching, Germany

Abstract:

The occurrence of high voltage electrical breakdowns between the ion beam extraction grids of a high-power neutral beam injector is one of the major factors that determine the performance of an injector. The tedious procedure of "conditioning" the electrodes in up to several thousand shots and the stressing of electrical supplies by the fast transients are two examples illustrating the need for more understanding of the actual origins of the high-voltage breakdown and the desire to reduce their frequency, thereby shortening the down-times of an injector. This report is an attempt to systematically address these questions. It starts with a survey of the relevant literature relevant to gap breakdown in the extraction optics system. Considering the various possible reasons for breakdowns, different methods for conditioning are discussed as to their potential effectiveness and with respect to the necessary effort. The proposed experimental work to improve the conditioning time will then be described. Finally the results so far obtained will be reported.

Index

1 Introduction

The commissioning of a multi-megawatt neutral beam injector (NBI) is usually a long and time-consuming business. One of the major contributors to this delay is the frequent occurrence of electrical breakdowns between the ion beam extraction grids. Typically the cleaned grids are first conditioned in vacuum and gas only conditions by spot knocking with a suitable high voltage supply up to their designed operating voltage. The second stage involves beam extraction whereupon the hold-off voltage of the electrodes in the presence of the extracted beam is found to be typically 25 - 50 % of the vacuum and gas only conditioned voltage. The system must now be reconditioned with the beam present; i.e. the voltage is reduced until stable operation can be achieved and then the beam voltage and current are increased in small steps following the perveance curve ($P = I/U^{3/2}$) with several breakdowns taking place at each new voltage level. This procedure is continued until the working voltage is reached. ($\approx$ 1000 - 2000 pulses) and thereafter the system gradually becomes more stable and tolerant to perveance mismatch. This beam conditioning procedure is found neccessary to a greater or lesser extent whenever the electrodes are handled or simply exposed to the atmosphere.

Examination of the electrode grids after successful conditioning reveals that most of the visible damage due to breakdowns occurs on the high field side of the decel electrode (cathode) as shown in Fig.1. The surface is characterized by many dull scarring tracks and fewer shiny spots ($\varnothing < 1$ mm). Since the copper electrodes were smoothly polished prior to conditioning, these observations imply that the new smoothly polished electrode surface is less suitable for ion beam extraction than a rough and damaged surface! As will be discussed later, however, on the microscopic scale it is possible that spot knocking removed or blunted sharp micropoints on the electrode surface which acted as suitable electron emission centres. Thus despite the damaged surface appearance, the electrode after conditioning has fewer microemission sites.

An observation on the ASDEX NBIs has been that if the injectors are kept under high vacuum for some months prior to conditioning then

the injectors are generally easier to condition. This leads to the suggestion that perhaps a water layer on the electrode´s surface is responsible for the electrode instability. Comparisons with molybdenum electrodes showed that whilst the general conditioning time for either material was not significantly different, Mo electrodes needed only to be under vacuum for a few days before conditioning could begin. From vacuum technology molybdenum is considered a more suitable material for vacuum applications than copper due to its lower outgassing rate. Since thermal buckling prevents baking of the electrodes it is possible that outgassing is a major contributor to the breakdown problem.

The production of a low divergent MW positive ion beam is usually achieved with a multi-aperture electrode extraction system, however, for the present study it is sufficient to consider the single aperture system shown in Fig. 2. The arrangement consists of a plasma generator and positive ion extraction optics and would normally be operated in pulsed mode to cope with the high power loads. The extraction optics consist of typically 3 electrodes which focus and accelerate the positive ions to 10´s keV where the second electrode, held at typically -3 kV, is used to focus the beam and prevent electrons backstreaming to the plasma source. Typical electrode spacings and operating voltages are indicated in Fig.2 and considering the voltage gradient across the electrodes it is assumed that breakdown events will only occur between the plasma and the suppressor electrodes where the maximum nominal field is $\approx$ 8 kV/mm. Surface flashover across the electrode insulation posts can be ignored, since the special mounting design ensures that electrode spacing is much less than the insulator length.

In a typical ion beam generator the system can be pumped out to $\approx 10^{-8}$ Torr before gas is admitted into the plasma source. During ion beam production considerable gas streams from the plasma source into the extraction optics and the pressure in the system is $\approx$ 5 mTorr. It is well known that the breakdown voltage, U_B, of the gap amongst others is usually a function of gas pressure due to the dependence of the ionization rate upon pressure. It is therefore essential to distinguish between breakdown events which occur between the electrodes

- in vacuum,
- at operating pressure but with no plasma production
- and finally during ion production.

This report starts with a survey of the literature relevant to gap breakdown in the extraction optics system. The problem of breakdown in the plasma source found in the periplasmatron will not be addressed here since not only are the more commonly used bucket sources comparatively quickly conditioned but also the rf source may replace such conventional sources. The proposed experimental work to improve the conditioning time will then be described. Finally any results so far obtained will be reported.

2 Vacuum and low-pressure breakdown initiation

2.1 Requirements for breakdown

Electrical breakdown occurs when the characteristic of an electrode gap changes from a high resistance insulator to a low resistance conductor and the current flowing in the gap circuit is limited only by the capability of the power supply. A transition from insulator to conductor therefore requires the presence of a conducting medium such as an ionized gas or metal vapour. In a vacuum it is clear that only gas desorption or surface melting of the electrode surface can provide this necessary medium. When gas molecules are present there is still the need for free electrons to ionize the gas. This chapter therefore discusses which physical processes can give rise to electron emission, gas desorption and electrode evaporation. Specific emphasis is placed on measurements and theories concerning vacuum gap breakdown, however, provided the electron mean free path is greater than the electrode gap spacing, it is reasonable to assume similar effects in low-pressure discharges will be present.

2.2 Field emission induced breakdown

2.2.1 The emission process

In gap fields > 10^3 - 10^4 V/mm one finds a more or less constant electron emission current, I, from the cathode; increasing the applied voltage, U, leads to a steady increase in the average current as shown in Fig. 3. Superimposed upon the current trace are microdischarges of duration ≈ 50 - 100 μs and magnitude up to 100 I_{av}. Such an I-U characteristic is measurable even when the electrodes are mechanically polished to 1/4 μm finish or electropolished and cleaned, fully degreased and assembled in a clean room. The emission originates from a few microscopic sites on the cathode surface and may consist of:

a) Metallic micro structures which locally enhance the electric field
b) Dielectric or semiconducting structures

Electron emission from metallic microstructures of size 10^{-2} - 10^2 μm is referred to as metallic field electron emission (MFEE) and occurs when the local electric field narrows the potential barrier at the surface of the emitter and allows electrons to tunnel through the barrier as shown in Fig.4. The emission current obeys a Fowler-Nordheim type law of the form:

$$j = C_1E^2 \exp(-C_2/E) \qquad \text{Fowler-Nordheim law}$$

where j is the current density, E the electric field, C_1 and C_2 are functions of the metallic work function, Ø. The onset field for field enhancements is ≈ $3 \cdot 10^6$ V/mm so field enhancements of 10 - 500 are required for MFEE. The exponential term is very sensitive to the value of the coefficient B[Ø] and hence the work function; e.g. emission current densities are a hundred times lower for the same microstructure geometry and external field for gold than for copper electrodes. Metallic emitters can emit currents of 10 - 30 mA steadily, i.e. current densities of up to 10^{12} A/m^2 can be carried without melting the micropoints. Microstructure can be formed during electrode polishing or more significantly by breakdown arcs and metallic particle transfer from the anode.

Non-metallic field emission (b) from dielectrics or semiconductors occurs when the field penetrates a micron sized insulating surface structure and tilts the energy bands such that field emission (tunnelling) occurs from the Fermi level in the metal into the bottom of the insulator conduction band as shown in Fig.5. These electrons are heated by the internal field enabling them to escape by Scottky emission over the low electron affinity barrier at the insulator / vacuum interface. Characteristic of such emission is a shift of the average electron emission to lower energies below the metal Fermi level. Non-metallic emission is assumed where no sharp geometric structures can be seen despite intense field emission. Similar cold emission involving small crystalites and resonance tunelling through H_2O molecules is also possible.
C deposits can also cause strong emission.

2.2.2 The ignition process

Field emission induced breakdown is generally assumed to be initiated by heating processes either at the anode (electron beam impact heating) or at the cathode (Joule and Nottingham effects). It is clear that as the temperature of a metal microemitter rises, so the resistance increases with a consequential increase in the Joule heating rate. Eventually the emitter melts or even explodes forming a microplasma at the cathode surface. Factors effecting the joule heating of a cathode microemitter are the material's resistivity, thermal conductivity, surface radiation losses and whether the Nottingham effect is cooling or heating the emitter. (The Nottingham effect is as follows: at low temperatures the emitted electron has less energy than its replacement conduction electron supplied at F_L whereas at high temperatures the converse is true and cooling results. The typical Nottingham inversion temperature is material dependent and for copper is $\approx$ 1500°C.)

The problem with the microemitter vaporization model for cathodic led breakdown is that microemitters can emit currents of 10 - 30 mA ($j \approx 10^{12}$ A/m^2) without melting yet sometimes a 100 nA current is sufficient for breakdown. It is believed that inhomogeneous gas adsorption (surface layer formation) can lead to non-

uniform current distribution at the emitter. Tests with air, acetone, CO and H_2O vapour have shown that the current instabilities increase dramatically and explain the superimposed pulsed currents in the I-U characteristic of Fig.3.

Breakdown initiation at the anode is generally considered in the literature to be less likely unless the anode melting point is much lower than that of the cathode. Although some authors postulate melting of the anode in gaps > 2 - 3 mm by FEE beams, anodic instabilities are not always sufficient for breakdown. 50 kV electrons striking a copper anode would penetrate ≈ 8 μm into the surface although their maximum rate of energy dissipation occurs at a depth of ≈ 300 - 600 nm. This can lead to explosive "bubble-like" anode processes giving rise to showers of molten microdroplets. It is concluded, however, that anode melting is a consequence of cathodic emission heating so field emission breakdown is really initiated at the cathode.

2.3 Microparticle (clump) initiated breakdown

2.3.1 Microparticle origins

Microparticles of size 0.1 - 10 μm can be present on electrode surfaces due to remnants from cleaning procedures, dust held on by Van der Waals forces or particles originating from thermal instabilities at either electrodes. Microparticles originating from thermal instabilities may be formed by either joule heating and melting of a cathode microemitter or electron beam heating of the anode giving rise to molten microdroplets which can later solidify on the electrode surface. It is clear that breakdown arcs can also be a source of such microparticles.

Although the microparticles are usually fixed to the electrode surfaces they can be detached by electrostatic forces. Prior to detachment the surface charge density on the microasperity depends upon the local microscopic field ($\sigma = \varepsilon_0 E$). The electrostatic detaching force ($F_d \approx Eq$) induces varying stresses depending upon the charge density and hence particle shape: a constricted stalk (illustrated in

Fig.6) being particularly vulnerable. Clearly the microasperities will become detached when the detaching force exceeds the retaining force, i.e. the material yield stress or Van der Waals forces. After detachment these microparticles (or clumps) will enter the gap as charged particles and be accelerated to high velocity towards the opposite electrode. Experimental evidence shows that such particles are frequently emitted prior to breakdown but in ≈ 97 % of all cases they travel from the anode to the cathode and the majority are < 1μm in size.

2.3.2 Breakdown ignition by microparticles

Experiments showed that the breakdown voltage could be reduced by up to 50 % when particles of ≈ 2 μm were deposited upon the electrode surface with a density of ≈ 10^7 m^{-2}; several mechanisms have therefore been proposed for microparticle initiated breakdown:

a) Evaporation in flight by electron bombardment.
b) Impact welding with subsequent field electron emission increase.
c) Evaporation on impact at the opposite electrode.
d) Trigger discharges between electrode surface and approaching particle.
e) Multi-transit impact phenomena.

For particles with low velocities (< 200 m/s) the most probable method of breakdown initiation is in-flight evaporation by electron bombardment as illustrated in Fig.7. As the particle is accelerated towards the cathode it travels into the electron beam path giving charge neutralization and rapid heating. At the limit the particle will vaporize midgap providing a conducting medium and permitting regenerative ionization processes. Clearly this mechanism is only effective for cathode particles. For particles with intermediate velocities (200 - 700 m/s) in-flight evaporation can occur or alternatively the particle can impact on the electrode leaving indentation microcraters or protruding microfeatures as illustrated in Fig.8. Such impacts upon the cathode can lead to enhanced field emission. Anode bound particles on the other hand lose charge

during transit by field emission and hence impact on the electrode with lower velocity and are consequently less dangerous. For particles with very high velocities (> km/s) in-flight evaporation can occur or alternatively the particle may impact the electrode with such force that it spontaneously vaporizes as illustrated in Fig.9. Particle vaporization gives rise to microdischarges and can therefore trigger breakdown. Note, however, that regenerative ionization processes must still occur for breakdown, so cathode-bound particles have a higher probability of initiating breakdown. It is worth noting that the breakdown condition is determined by the voltage across the gap rather than the field.

Microdischarges can also be triggered between the electrode surface and the approaching particle due to the local image charge field enhancement as illustrated in Fig.10. Experimentally breakdown has only been found to occur in this manner with large particles

(> 100 μm) probably because the charge density on smaller particles is too low to cause sufficient field emission and subsequent material vaporization or gas desorption before the particle arrives at the electrode.

The final possible method of initiating breakdown by microparticles is by multiple transits of the particle (bouncing) across the gaps as illustrated in Fig.11. At voltages below the breakdown voltage of the gap, particles can bounce between the electrodes and give rise to a measurable current. This phenomena occurs for sub-micron sized particles and energy enhancement can occur by several particle transits between the electrodes. The method requires an efficient reversal of both particle momentum (coeff. of restitution -> 1) and charge (resistivity -> 0) to ensure that the particle leaves the electrode with high velocity and will be accelerated to the opposite electrode. Clearly particles with conduting or semi-conducting surface layers will be much more likely to undergo multi-transit phenomena. When the particles have gained sufficient energy then one of the other microparticle breakdown initiated mechanisms described earlier can occur.

2.4 Transition from ignition to breakdown in vacuum

Typically a micron-sized plasma cloud (cathode spot or flare) is formed near the cathode by one of the ignition mechanisms described earlier, as illustrated in Fig.12. Region 1 in the diagram is the space charge zone of thickness ≈ nm between the plasma and the electrode surface. Region 2 is the luminous plasma spot of size 30 - 50 μm and particle density > 10^{23} m^{-3}. The voltage drop across the cathode fall between the spot plasma and electrode surface is ≈ 50 V so very high currents can flow through Region 1. Outside the dense plasma there is a less luminous plasma in Region 3 which expands with a velocity 10 - 20 mm/s such that the density decreases inversely with the square of the distance to the spot centre. The voltage drop across Regions 2 / 3 is negligible because of the high plasma conductivity. In Region 4 there is vacuum so the gap must be bridged by random electrons emitted from the edge of the plasma in Region 3. The potential across Region 4 is approximately equal to the gap voltage so high energy electrons impact the anode and form anode flares which intercept the cathode plasma and breakdown follows.

The decision whether breakdown was initiated by MFEE or by microparticles has been determined experimentally as follows. For small gaps (< 2 mm) MFEE is the dominant breakdown mechanism and thus depends upon the average field and the local fields in the gap. For larger gaps (> 5 mm) the dominant breakdown mechanism appears to be microparticle based ignition which depends upon the voltage across the gap rather than the field. It must, however, always be remembered that field electron emission from the cathode is necessary for breakdown even when microparticles are released from the cathode. This is why it is often reported that the breakdown is initiated at the cathode especially with well conditioned electrodes, since anode melting leading to anode plasma formation prior to cathode spot formation is unlikely. It is though likely that MFEE from new electropolished electrodes will take place by non-metallic field emission until either the oxide layer on the electrode surface is removed or alternatively microparticles are formed after arcing providing other emission sites.

2.5 Effect of gas admission and desorption

Paschen's law states that the breakdown voltage of a uniform field gap is a unique function of the product of pressure and electrode spacing for a given gas. The minimum breakdown voltage occurs for a specific $(p.d)_{min}$ and at lower and higher product values the breakdown voltage increases. This can be explained qualitatively as follows: if the gas density and/or the gap spacing decreases then the electrons will arrive at the anode before ionizing the $\approx 10^8$ ions required for breakdown; if the gas density and / or the gap spacing increases then the average energy gained from the field between collisions will be insufficient for ionization. In the present investigation Paschen's law is not applicable to predicting the sparking voltage of the gap for the following reason:

a) Electrode effects cannot be ignored.
b) Swarm conditions are not existing.
c) Hydrogen appears not to have a unique dependence upon (p.d).

Considering these points individually it has been shown that the effect of surface protrusions and microplasma formations is crucial to breakdown formation in vacuum, so it is clear that provided the gas pressure is comparable to the local metal vapour or gas desorption pressure formed prior to breakdown, then these latter effects must also be considered. Secondly Paschen's law usually assumes that the electrons drift with a uniform average drift velocity such that the reduced ionization coefficient is a unique function of the reduced field. In the present situation the mean free path between collisions is longer than the gap spacing so the electron velocity distribution is far from uniform and the collisions are not thermal (< eV). Finally Fig.13 shows the results of breakdown measurements by Guseva (1964) which demonstrates the unusual effect that U_B is not a unique function of p.d since this result clearly shows a strong gap dependence. The only use of this curve for the present work is to indicate that, since the usual operating conditions of the neutral beam injector are $p.d \approx 4 \cdot 10^{-3}$ Torr cm, it is clear that we are dealing with breakdown events far on the left hand side of the Paschen curve. Further evidence that U_B is not a unique function is given in Fig.14 where U_B shows a strong

dependence upon gap spacing but not upon pressure for pressures < 1 mTorr. In larger gaps (≈ 8 mm) and normal ion beam operating pressures (5 mTorr) it is apparent that U_B decreases due to the increased pressure but no measurements are available for the increased gap spacing. It is expected that the hydrogen admission will reduce the breakdown voltage of the gap compared to vacuum since the gas is an ionizable medium, however, at such pressures the effect may be small.

If an oxidizing gas is used such as O_2 it is possible to increase the work function of the metal surface, e.g. for copper, stainless steel and molybdenum by 0.3 - 1.8 eV. For a small range of pressures U_B can actually increase with increasing pressure. This occurs not only due to the increased work function of the electrodes but also due to the increased surface resistance of oxide so that charge transfer during multi-transit phenomena is restricted. Additional increases in the oxide melting temperature may also explain this stand-off voltage increase. Experimental evidence in small gaps (≈ 0.5 mm) has shown that the pre-breakdown current of a gap increases with H_2 pressure over the range 10^{-7} - 10^{-3} Torr but at higher pressures (> 5 mTorr) the current dramatically decreases as illustrated in Fig.15. It was suggested that at such pressures ion bombardment of the cathode removed a film of adsorbed H_2 and so increased the work function. There is, however, little evidence to show that Ø[eV] changed and it is more likely that the ion bombardment simply blunted the microscopic emitters.

2.6 Effect of ion beam

The most obvious effects of the positive ion beam on the breakdown voltage of the electrode gap are as follows.

a) Gas desorption by ion beam heating of the electrode surface
b) Secondary electron emission (SEE) by high energy beam impact on the electrode surface
c) Electric field distortion by ion beam space charge
d) Impurity production and metallic transfer from the source

It is reasonable to suppose that despite well designed ion beam optics a small proportion of the high energy ions will not pass

through the cathode (electrode 2) but instead will impact upon the electrode surface. Such ions can penetrate ≈ 10's nm into the surface and dissipate their energy either as heat or quantum transfer leading to SEE. The intense heating of the electrode surface will promote not only trapped gas desorption but also thermionic emission. The SEE coefficient for 40 keV hydrogen ions impacting on copper is 1.2 - 1.7, so large numbers of electrons could be released into the gap by ion impact. It is worth noting that the electrode work functions are typically 4 - 6 eV so it seems very unlikely that SEE production is effected by the electrode material. By contrast the electroode thermal conductivity and adsorbtivity must have a significant effect on gas and electron emission.

Whether the ion beam charge density (10^{14} - 10^{15} m^{-3}) is sufficient to distort the electric field is not clear but the probable answer is no provided the ion beam is being operated at optimum perveance. Finally the effect of impurity production from the source may have an effect on the breakdown voltage. It is known that metal vapour is transported along the beam as well as other high Z particles; all these may impact the cathode giving increased electron emission and gas production. It should be remembered that gas production only needs to be high in localized regions where field electron emission is already present for breakdown to be initiated. Finally, high energy ions can activate field assisted surface diffusion of contaminant atoms from the shank of the emitter; this can promote crystal growth through the self diffusion of surface metal atoms to form microprotrusions.

3 Electrode material choice for maximizing U_B

It is well known from breakdown studies of vacuum gaps that electrodes constructed from copper or nickel are often subject to instabilities having comparatively high pre-breakdown currents and more frequent breakdown events at lower voltages. In contrast materials such as stainless steel (SS), Ti and perhaps molybdenum are very stable materials for vacuum gap electrodes; how can this be explained?

Hardness

Copper and nickel are soft metals compared to SS etc. but so is tungsten steel and the latter is very unstable; nevertheless there is less chance of microparticle damage to the electrode surface forming microcraters and hence MFEE sites since for metal vapour production $v_{Mo} \approx 5$ km/s compared with $v_{Cu} \approx 1.5$ km/s.

Corrosivity

The stable materials are very corrosion resistant especially after oxidation since they have hard oxide layers of ≈ 5 nm thickness. Furthermore SS oxide layer is a strong insulating ambient film compared to the semi-conducting oxide layer of copper. This means that non-metallic FEE as well as multi-transit phenomena are unlikely for SS etc.

Vacuum fitness

The stable electrode materials are suitable for UHV equipment unlike copper. This means that outgassing (gas desorption) may play an important role in initiating breakdown.

Melting point

The melting point of copper is 1084°C compared with 2620°C for molybdenum so metal vapour production from copper occurs at lower temperatures. Furthermore the Nottingham inversion temperature is $\approx$ 1500°C so only Mo can experience cooling.

Electrical conductivity

Copper is an excellent electrical conductor compared with other metals (resistivity is ≈ 3x less than for Mo at 500°C) so Joule heating is lower so conductivity appears not to effect electrode stability.

Thermal conductivity

The thermal conductivity of copper is very high (factor 3x compared with Mo) so heat dissipation in copper is more effective. This is apparent when measuring the time-to-breakdown of a vacuum gap: Mo is much quicker.

Work function

It has already been stated that MFEE onset is strongly dependent upon the surface work function. Ion beam bombardment of the electrode surface with keV ions will, however, produce SEE from all surfaces since $\emptyset_{metal} \approx 4 - 6$ eV. It is interesting to note that $\emptyset_{Cu} > \emptyset_{Mo} \approx 4.6$ eV so Mo stability is not connected with the work function.

Surface layer

Various coatings have been tried on electrodes e.g. Si, CaF_2. These coatings were of ≈ μm thickness and applied epitaxially (fused) onto the surface of sub-mm gaps and were successful at reducing both the pre-breakdown current as well as increasing the breakdown voltage, (Smith 1986). A single breakdown event, however, destroyed the benefits and made other conditioning methods ineffective afterwards due to removal of part of the coating layer.

Anode-cathode difference

The anode surface particles are preferentially transported to the cathode during pre-breakdown events so a soft low melting point metal such as copper for the anode would be useful to reduce the formation of microcraters on the cathode surface. In contrast the cathode should be hard with an insulating oxide layer and very high melting point.

4 Electrode conditioning

The most common methods of conditioning vacuum and low pressure electrodes in increasing order of effectiveness are as follows:

1) Electrode heating
2) Glow discharges
3) Pre-breakdown current
4) Spark knocking

Electrode heating to high temperatures (ideally > 1500°C) will outgas the surface and enable the surface microstructure to flow in order to minimze its surface energy; note that the cooling rate is important. At lower temperatures (300°C) the electrodes will simply be outgassed. The problem with this technique is that the NBI electrodes cannot be heated to such temperatures without causing severe mechanical distortion.

Glow discharges are often used to clean electrode surfaces of oxide layers etc. and also to blunt electrode micropoints by sputtering action. There is no general agreement as to which gas, at what pressure and what current density are most appropriate. Typically, hydrogen and helium are used for fusion devices whereas argon is used for particle accelerators, since any residual high-Z argon is not a problem in this latter application. In tokamaks Dylla (1989) claims that H_2 discharges are more effective than He in removing impurities from SS walls, however, with carbon coated walls both gases are effective although He tends to only remove a surface monolayer of impurities. In contrast Latham (1981) summarized earlier work by different authors and suggests that He is the most effective gas for conditioning of point-plane electrodes. It appears that hydrogen can react more easily with surface oxide impurities leaving an electrode surface clean, whereas helium is more effective at sputtering the micropoints on the surface due to its higher atomic mass.

The approximate ignition voltage observed by Dylla in the Princeton tokamak is 300 V[He] and 400 V[H_2] for an operating pressure of ≈ 5 mTorr. Considering the large dimensions involved in a tokamak

and hence long mean free path (m.f.p.), the necessary gas pressure in the present 7 mm gap will be ≈ 100x larger. The current density, j, is usually adjusted to be in the range 10 - 25 $\mu A/cm^2$ by varying the applied voltage since the discharge is run in the abnormal glow regime. If $j < 1\ \mu A/cm^2$ the glow will normally extinguish and if $j > 100\ \mu A/cm^2$ an arc may form. The glow discharge is often run for several hours although it is possible to overcondition the electrodes leading to degradation in performance so regular testing of the condition status is required during the discharge. Inital tests on the HF PINI Teststand showed that glow discharges of duration < 4 hours produced no significant improvement in the condition state, however, with a 12 hour discharge there was a transient improvement but after each ion beam pulse the number of breakdowns increased until after only 5 pulses the original deconditioned state was obtained. The improvement was slightly more marked with He than with H_2.

Pre-breakdown current conditioning is suitable for virgin electrodes especially if they are to be used in passive applications. Probable explanations for its effectiveness are that the sharpest field emitting microprotrusions are either thermally blunted from excessive emission or if mechanically unstable then removed from the electrode by strong electrostatic forces. Particles are always detached at the lowest possible fields and hence aquire minimum charge; explosive impact breakdown is therefore highly unlikely. Field desorption of trapped gas in grain boundaries is also possible. Breakdowns in an NBI will probably be impossible to totally eradicate so this method is not considered suitable. Note that none of the methods described so far has any effect on microparticle initiated breakdown which we have already said is the dominant process in gaps > 5 mm.

Spark conditioning (syn. spark knocking) is particularly effective at removing localized high field electron emitting sites on the cathode by arc erosion (melting) as well as eliminating microdischarges and dimishing microparticle processes. The method may also cause local hardening of the surface near emitting regions but it is essential that the total dissipated energy is < 10 J to prevent electrode damage. Spark knocking is generally agreed in the

literature to be the most effective means to condition vacuum gaps, however, it should be remembered that in nearly all the reported tests the electrodes had been thoroughly outgassed by baking to several hundred degrees Celsius prior to conditioning; an option which is not possible to realize with the NBI electrodes. Furthermore, as mentioned in chapter 2, it is already common practice during the early stages of NBI conditioning to condition the electrodes by spark knocking in vacuum and gas only conditions up to 65 - 100 % of the planned maximum extraction voltage, U_{max}. Typically < 5 % of the complete conditioning time is required for this procedure before the gap reliably holds the maximum designed voltage, Nevertheless, as soon as beam extraction is attempted breakdown occurs at much lower voltages. It is therefore essential that the spark conditioning voltage exceeds the maximum normal extraction voltage; this could present problems with the existing HV insulation structure.

5 Other effects

In the bulk of this report the reasons for breakdown between 2 electrodes have been discussed in terms of the well documented vacuum breakdown physics. It must be remembered though with an NBI that other factors will effect the voltage withstand ability of the electrodes. In particular the impurity production from the plasma source and the non uniformity of the same source. Considering these factors separately:

1) The plasma source generates enormous heat and consequently substantial outgas impurities which will be affected differently by the electrostatic lens of the extraction optics and could thus impinge on the decel electrode causing SEE. The protron yield of the source is never 100 % but more typically ≈ 85 % which means a large number of lower energy ions and neutrals are still streaming through the source grid and can impact on the decel electrode.

2) The production of a large area uniform density plasma for the NBI is essential for minimal beam divergence as well as being an essential requirement for a high gap withstand voltage. This is because the ions distort the electric field in the gap since they resemble a conducting channel and unless the plasma current is perveance matched to the accelerating potential, breakdown will occur due to incorrect focussing.

6 Experimental work

The aim of the initial experimental stage is to test whether conditioning of the electrodes alone by glow discharges and/or spark knocking with voltages > U_{max} reduces the time required to condition the electrodes. If no significant effect is observed then either the effect of cathode coatings in the electrode surface must be investigated or a more general study of the dependence of the electrode hold-off voltage upon the rest of the NBI must be undertaken. This latter study would involve considering effects such as embedded impurities in the NBI materials such as in the insulation walls and plasma ion source as well as the uniformity of the ion source itself.

We shall define an electrode condition factor, F_B, to quantify the conditioning status of the NBI as compared to a fully conditioned injector generating a 1 s duration ion beam at the maximum designed extraction voltage. That is:

$$F_B = 100 \times \int_0^1 \frac{U_{acc}}{U_{max}} dt \quad \%$$

where F_B ranges from 0 (unconditioned) .. 100 % (fully conditioned). Although F_B appears to mask the number of breakdowns during the 1 s pulse it must be remembered that the arc-knotching time is $\approx$ 50 ms which will significantly reduce F_B.

In order to determine whether a particular new-conditioning procedure is effective it is clearly necessary to start with a benchmark

for normal conditioning. In other words we need to obtain a graph of F_B vs. number of pulses, N_P, for the standard conditioning procedure. It is planned to perform all the experiments using the old ASDEX NBI, driving the NW Quelle 1 beamline. This benchmark determination will also provide time for recomissioning of the system. After the first conditioning run it is necessary to test a simple but effective deconditioning method. It is proposed to use humid air admission for this purpose. The first experiments will therefore look as follows:

Experiment 1: Benchmark

1) Condition injector recording F_B vs. N_P
2) Decondition injector with humid air
3) Repeat stages 1) and 2) once more

Provided there are no major discrepancies between the two benchmark plots it is possible to move onto Experiments 2, 3 (testing of the new conditioning procedures). These experiments will occur as follows:

Experiment 2: Glow discharge

1) Run glow discharge in H_2 for (1,2,4,8,16 hrs)
2) Measure F_B after each discharge
3) Repeat 1 - 3 for new conditioning time
4) Decondition electrode
5) Repeat steps 1 - 4 using He

Experiments on the HF teststand have shown that the operating regime (i.e. pressure, current density) for the glow discharge is remarkably small so the parameters given earlier in this report will be adherred to. High gas pressure may be tested at a later date with consequential reduction of the ignition voltage. Note that a current limited power supply (AC or DC) with output variable up to 1 kV is required.

Experiment 3: Spark knocking

1) Increase U_{acc} until breakdowns occur
2) Leave running until breakdowns cease
3) Repeat steps 1) and 2) until $U > U_{flashover}$
4) Measure F_B
5) Repeat stages 1 - 4 with different HV interrupt delay time (T_B -> T_{off}) and thus spark energy

The aim of this experiment is to condition the electrodes in vacuum or gas only conditions up to $U > U_{max}$ despite the limitations of the HV insulators. Further account must also be taken of the leakage current through the water cooling connections when choosing a power supply for the experiment. After discussions with H. Melkus it appears that the HV Anlage can be run in continuous mode since the current drawn is very low; a manual reset is required if the number of breakdowns exceeds 99. A greater problem is the HV cable whose transmission voltage should not exceed 60 kV. This limits the applied sparking voltage to only ≈ 10 % greater than the normal conditioned voltage so little benefit can be expected here. Alternatively a separate power supply is required and the electrical and water connections must be removed. It is unlikely that the ASDEX injectors can cope with extraction voltages > 70 kV. Only if tests are made on the JET-PINIs can higher voltages be used.
A possible option to overcome the insulator charging prior to breakdown by flashover may be to use a sparkgap in series with the HV cable. Sharp HV pulses of short duration would be applied at a significantly higher voltage than U_{max}.

7 Experimental results

The NBI machine was used on 11 experimental days as shown in Table 1. Despite this short period the injector was conditioned to 50 kV, 18 A, 1 s extracted beam and then reconditioned after exposure to humid air.

Date	Pulses	Primary job
2/9/91	100-152	System checks, arc conditioning
3/9/91	153-174	Arc conditioning
4/9/91	175-247	Beam extraction (T_P = 300 ms)
5/9/91	248-360	Beam extraction (T_P = 1 s)
6/9/91	361-410	Beam extraction (T_P = 1 s)
19/9/91	411-462	Beam extraction (T_P = 1 s)
20/9/91		Injector exposed to humid air (h_r = 60 %, 20°C) for 2 hrs
20/9/91	463-495	Beam extraction (T_P = 1 s)
23/9/91	496-564	Beam extraction (T_P = 1 s)
26/9/91	465-580	Beam extraction (T_P = 1 s)
27/9/91	581-595	Beam extraction (T_P = 1 s)

Table 1

On each experimental day prior to beam extraction or when a pause >30 mins between pulses occurred the periplasmatron ion source was conditioned for 3 - 10 pulses with at least 2 pulses generating an ion current >350 A for 1 s. Breakdowns in the arc supply were not observed during this procedure and it was thought that such pulses warmed and cleaned the system. This procedure was also used to restabilize the system whenever 2 or more ion extraction pulses suffered breakdowns in the electrode gap. Although the extraction voltage was also reduced after such breakdowns this alone was found insufficient to stabilize the gap.

In order to keep the thermal and electrical power loads on the injector to safe limits, the maximum extracted energy aimed for was ≈ 870 J (50 kV, 18 A, 1 s). Figure 16 shows how the extracted energy varied with shot number and it is clear that the maximum energy was achieved remarkably quickly (< 200 extraction shots). This suggests that either the injector was already well-conditioned

or alternatively the high power arc discharge prior to extraction helped stabilize the gap. The former reason is possible since the injector was exposed to air whilst repairs were carried out on the injector chamber, however, the electrodes were never disturbed. Between shots 200 and 564 there are clear regions in Fig.16 where no extraction occurred. This was deliberate and occurred when the author wished to perform arc-conditioning without beam extraction. Apart from a very small minority of pulses (< 20) a shot showing no extracted energy did not undergo breakdown but was simply an arc-only pulse. Pulses 411 - 462 show how the arc current was conditioned before the extraction voltage was gradually increased. 5 interrupts were observed during this run until it was realized that the arc current was set too high.

After pulse 462 the gate valve between the injector and the main injector box was closed and humid air (h_r = 60 %, 20°C) was admitted into the injector. After 2 hrs exposure to atmospheric air the injector was pumped down externally to ≈ 0.1 Torr before the gate valve was reopened. A few arc conditioning pulses were made before extraction was attempted again. More than 700 kJ could be extracted within 20 pulses despite the electrode exposure to air. The following day maximum power could be quickly achieved after arc conditioning despite 2 breakdowns occurring whilst attempting to increase the extracted current too rapidly. If the midday pause around pulse 530 is ignored full extracted power was achieved and maintained quickly (< 25 pulses) suggesting that short term exposure to humid air has no effect on the conditioning state of the gap.

Figure 17 shows how the condition factor varies with shot number and apart from low values whilst arc conditioning or an interrupt occurred, F_B clearly exceeded 90% for most of the shots illustrating again that breakdowns were not a problem. Comparing Figs.16 and 17 it would appear that although F_B exceeds 90 % the extracted energy is well below the derived value for many of the pulses. This is because F_B does not depend on the extracted current unlike the beam energy and although the author planned to increase I_{acc} with

U_{acc} according to the perveance curve this was not achieved. Instead it was found easier to achieve reliable operation by driving the injector at lower currents than demanded by perveance until the full extraction voltage had been reached.

8 Discussion

A novel method for reducing the conditioning time has not yet been tested, however, experiments have been performed to derive a benchmark timescale for standard conditioning. Furthermore an initial attempt to decondition the electrodes has been tested albeit unsuccessfully. Graphs showing how the beam energy and electrode condition factor vary with pulse number have been presented, however, fundamental problems are visible. The breakdown voltage of the gap when ion extraction occurs depends on more factors than originally appreciated by the author. Amplitudes of the arc current, electrode temperature, decel voltage, gas input rate, background vacuum pressure, injector history all appear to have a significant effect on the condition status of the injector. Furthermore, if effects such as full power arc-only conditioning also benefit the conditioning time, how can this and other effects be considered when comparing two graphs of F_B vs. pulse number for two different injectors or when the injector is specially treated prior to conditioning? Clearly it if were possible to switch-on the injector and immediately obtain full power then the conditioning time would have been illiminated. In the grey area where a small improvement in conditioning time is perceived after a particular pre-conditioning handling process, it is difficult to tell whether some other factor caused the improvement. This problem remains wide open to discussion.

The fact that admission of humid air into the injector for 2 hrs did not decondition the injector is not proof that were air admitted for a longer period ($\approx$ month) an effect might have been seen. That prolonged pumping of the injector prior to conditioning is known to

improve the ease of conditioning suggests that exposure to air for a similar period would have the converse effect. In other words, trapped gas and outgassing are important factors to be considered when conditioning an injector. The need to find a simple but effective method to decondition the injector still remains though!

An important question which must be answered is whether breakdown in the electrode gap occurs primarily as a result of the electrode surface properties or of the vacuum quality and applied settings (e.g. U_{dec}). Electron emission necessary for breakdown initiation will occur both from FEE and SEE so to isolate the primary cause for breakdown is not easy, especially with so little experimental data. The author hopes that this preliminary report will spur someone else to persue the problem further and enable these important questions to be answered.

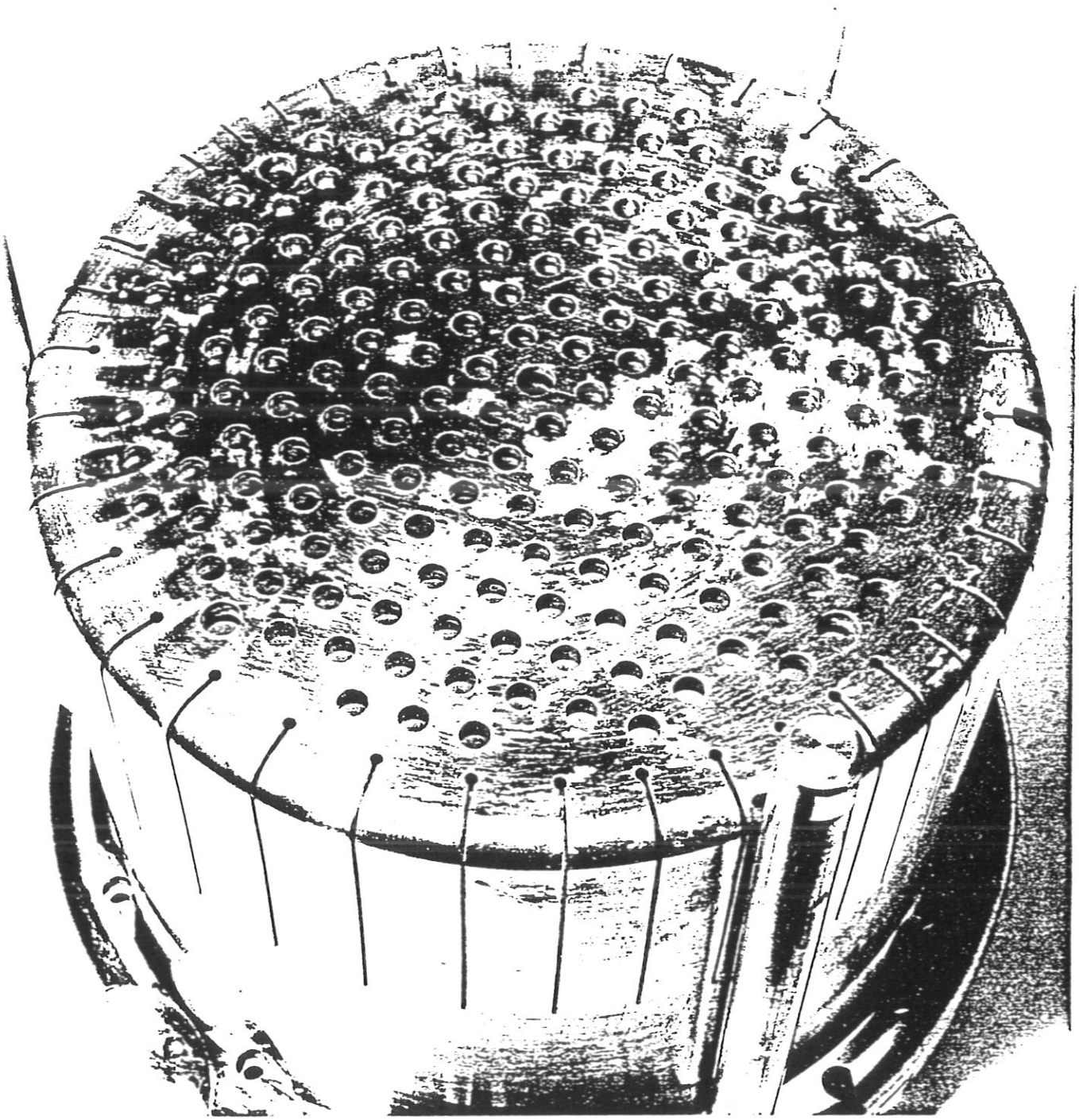

Fig.1 Surface damage on the high field side of the ASDEX suppressor electrode after conditioning

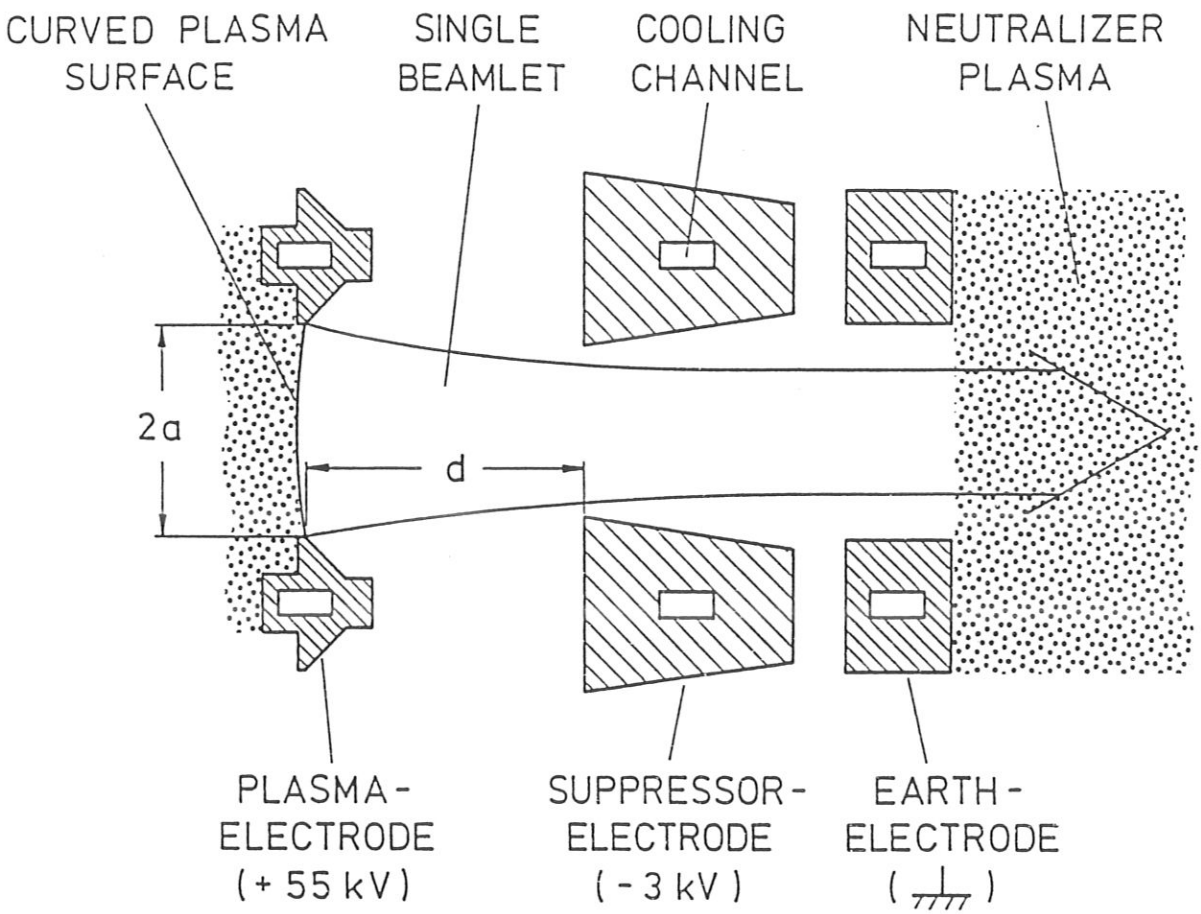

Fig.2 Schematic of single aperture ion extraction electrodes, (Speth 1989)

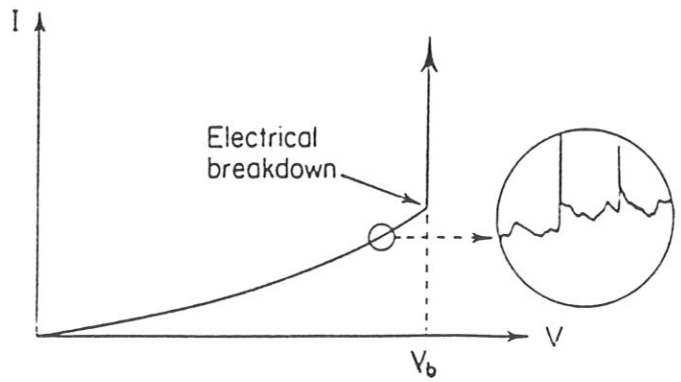

Fig.3 Typical form of the non-ohmic I-V characteristic of a high voltage vacuum gap, (Latham 1981)

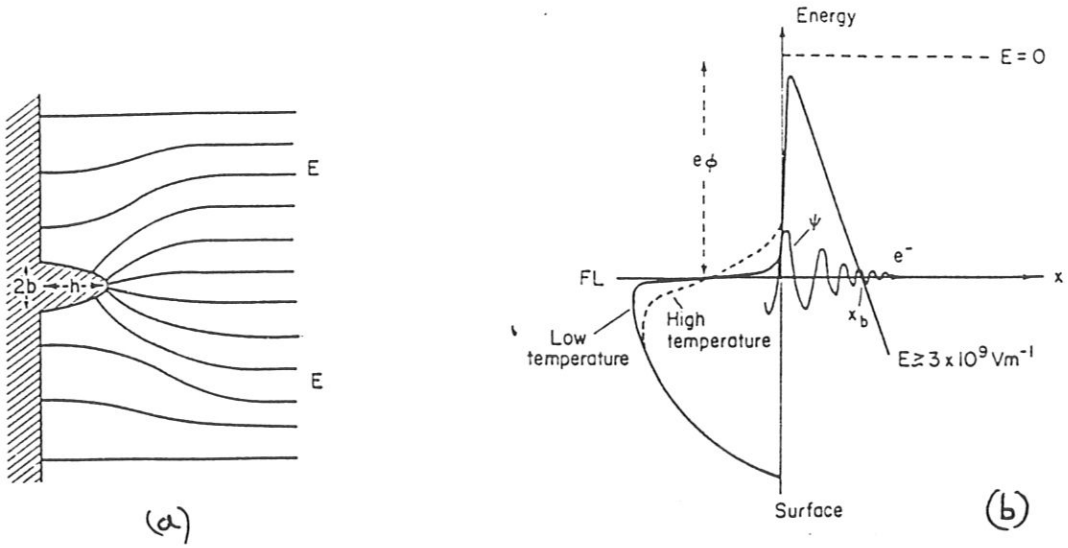

Fig.4 MFEE: a) local field enhancement at the tip of a microprotrusion; b) Quantum mechanical tunnelling mechanism for MFEE, (Latham 1981)

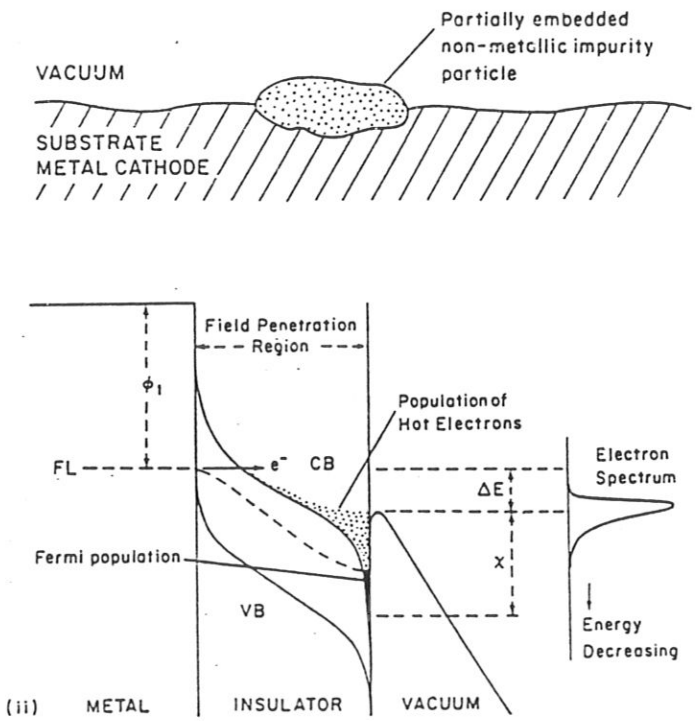

Fig.5 Non-metallic FEE: a) the microregime believed responsible for emission; b) Quantum mechanical tunnelling into the insulator followed by schottky emission into the vacuum, (Latham 1981)

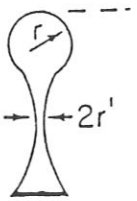

Fig.6 Constricted stalk particularly vulnerable to electrostatic detachment leading to formation of microparticles

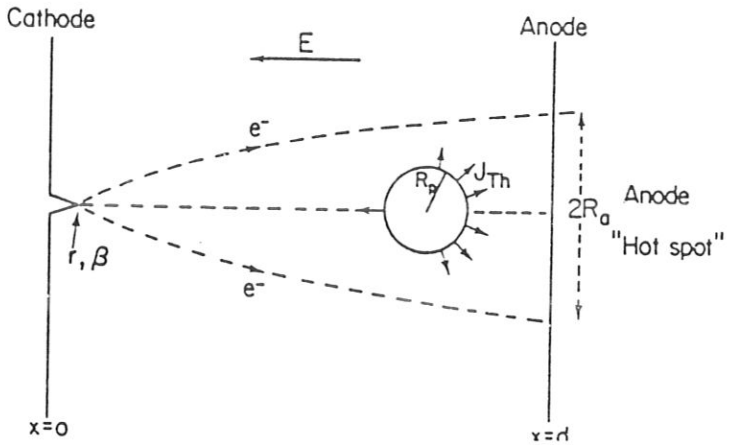

Fig.7 Schematic illustration of the heated anode particle breakdown model, (Latham 1981)

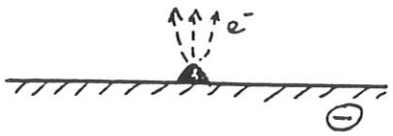

Fig.8 Microcrater formation leading to enhanced FEE (v = 200 -700 m/s)

Fig.9 Microparticle evaporation by impact (v > km/s)

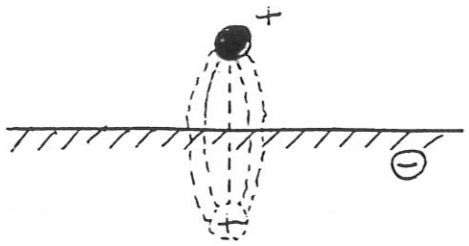

Fig.10 Discharge trigger by image charge field (Ø > 100 µm)

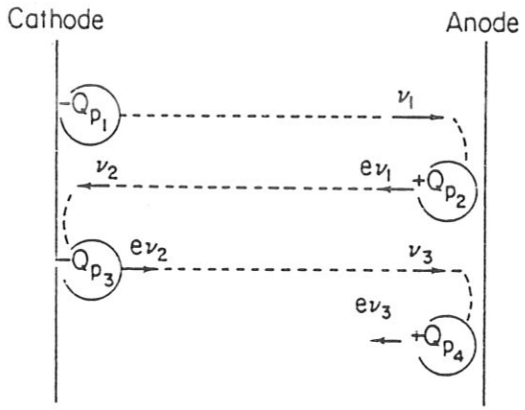

Fig.11 Kinetic energy enhancement model illustrating microparticle bouncing impacts with associated momentum and charge reversal, (Latham 1981)

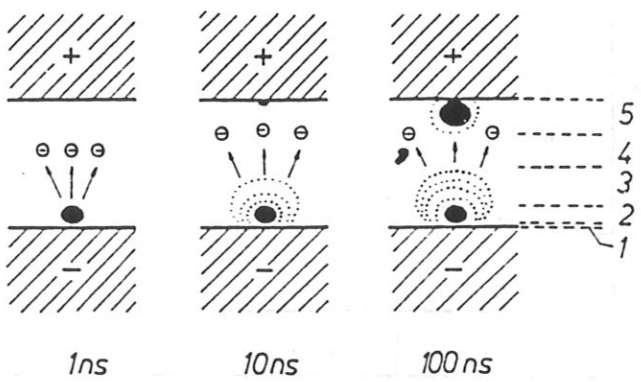

Fig.12 Different regions of a vacuum gap during breakdown: 1) space charge sheath; 2) plasma flare; 3) expanding plasma; 4) vacuum zone; 5) anode flare, (Jüttner 1988)

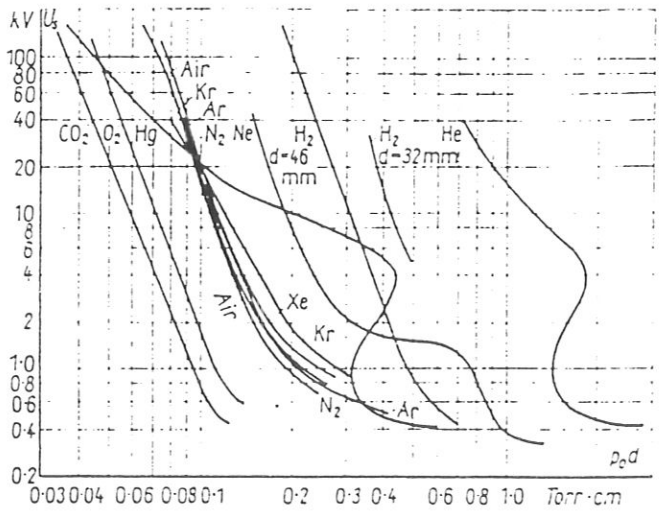

Fig.13 Left hand sections of Paschen's curve for different gases, (Guseva 1964)

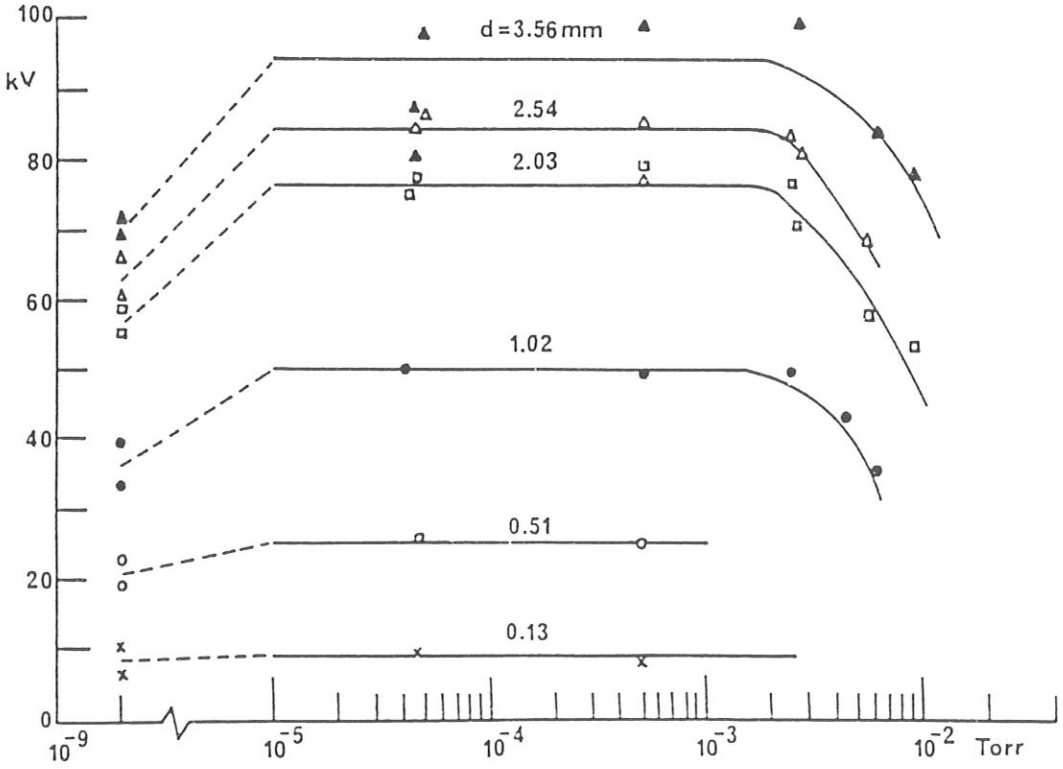

Fig.14 V_B as a function of H_2 pressure for various gap lengths using copper electrodes, (Altcheh and Hackam 1974)

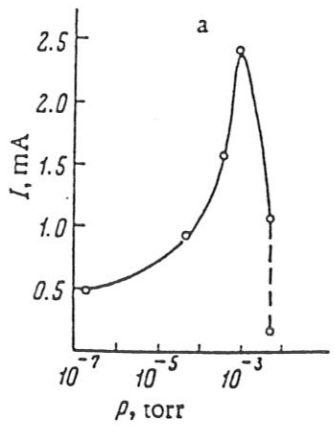

Fig.15 Dark current as a function of H_2 pressure at V = 19kV, (Potsar and Tyurin 1976)

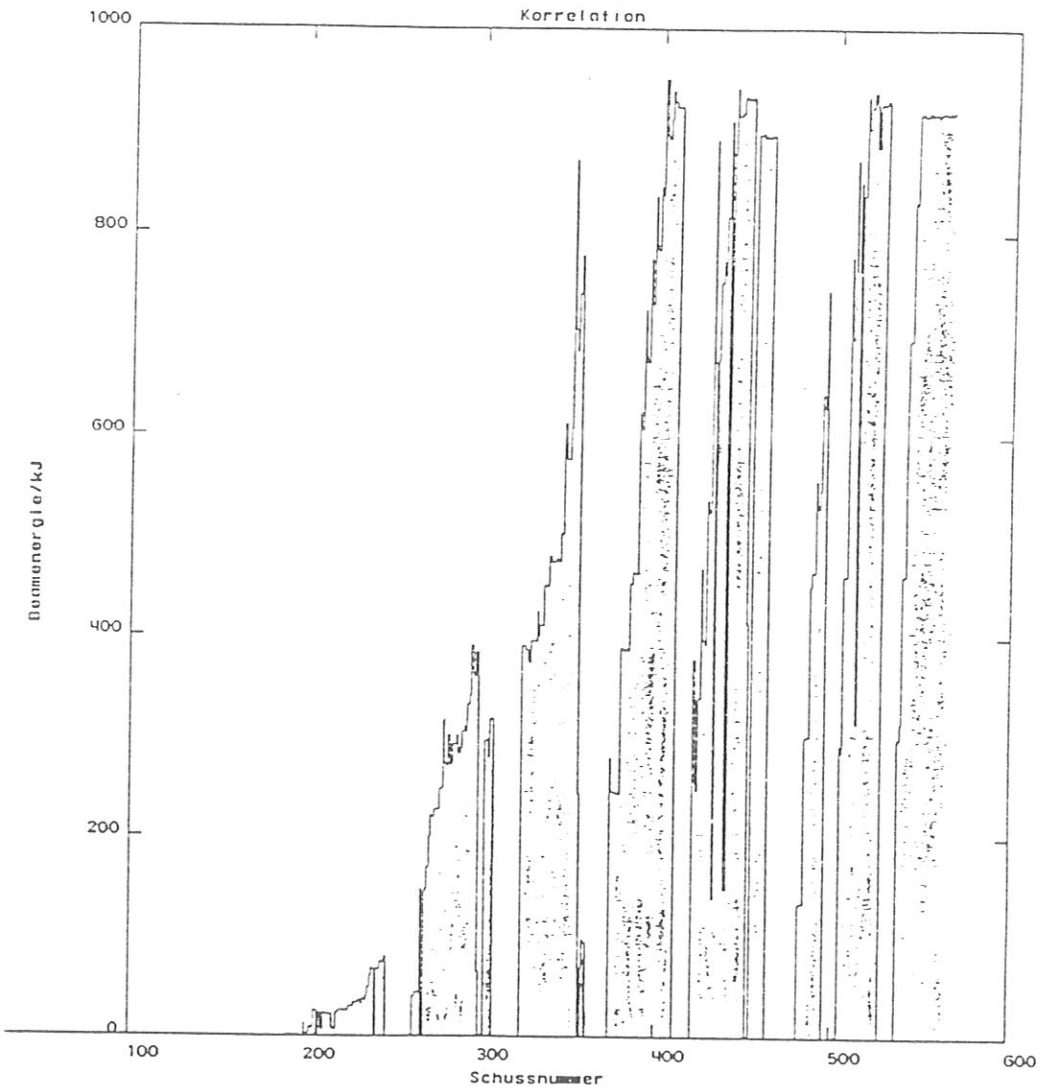

Fig.16 Variation of ion beam extracted energy with shot number

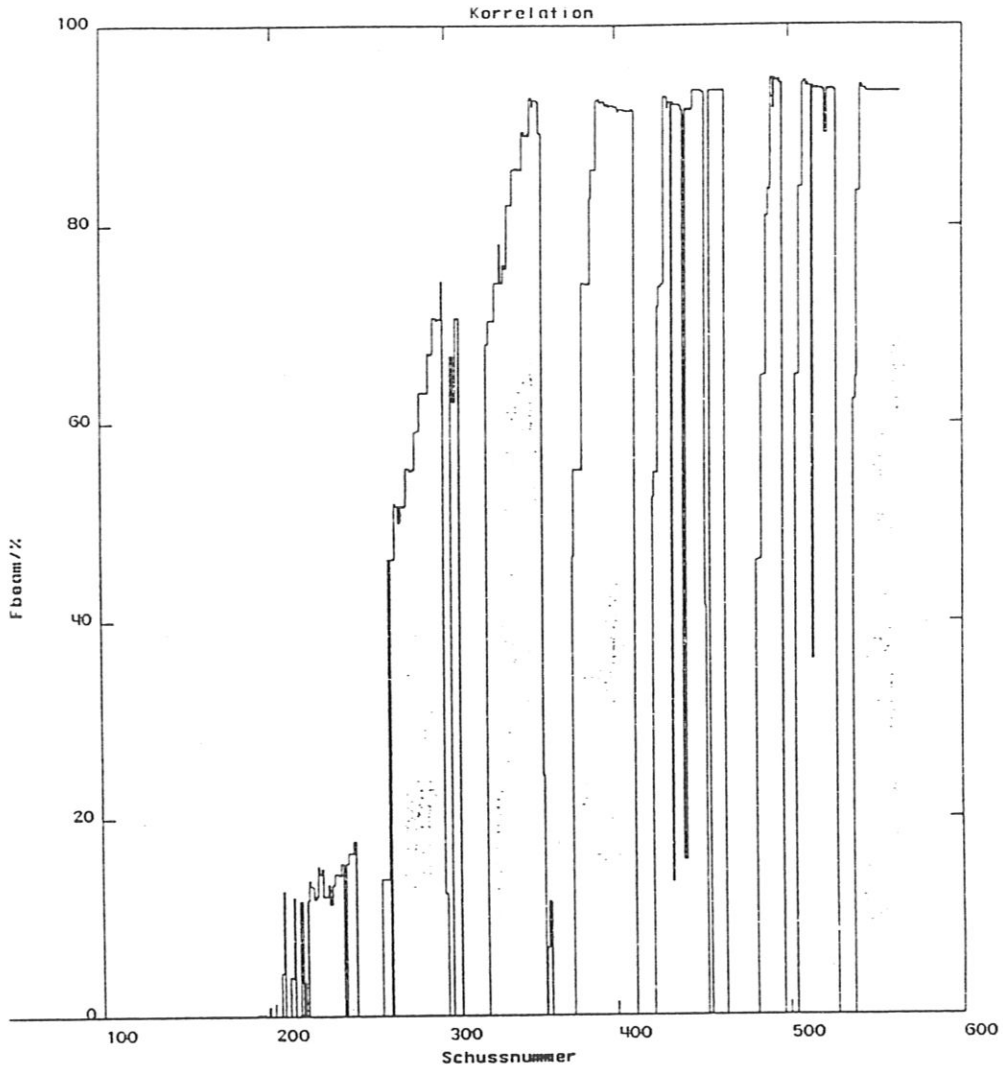

Fig.17 Variation of condition factor with shot number

REFERENCES

Altcheh, H. and R. Hackam (1974). Effects of additional hydrogen on the electrical properties of ultrahigh vacuum gaps using OFHC copper and nickel electrodes. *Proc. 6th Discharges and Electrical Insulation in Vacuum (D.E.I.V.)*, Swansea 1974. p.71-6.

Dylla, H. F. (1989). A comparison of hydrogen vs. helium glow discharge effects on fusion device first-wall conditioning. Report *Princeton Plasma Physics Laboratory* 2642.

Guseva, L. G. (1964). On discharge striking in polyatomic gases at pd < $(pd)_{min}$. In: *Investigations into electrical discharges in gases* (ed. B. N. Klyarfeld'd) Pregamon Press, Oxford. p.1-11.

Jüttner, B. (1988). Vacuum breakdown. *Nucl. Instrum. Meth. Phys. Res.* A268, p.390-6.

Latham, R. V. (1981). High voltage vacuum insulation: the physical basis. Academic Press, London.

Potsar, A. A. and I. P. Tyurin (1976). Field emission at low hydrogen pressures. *Sov. Phys. Tech. Phys.* 21 (5), p.631-2.

Smith, J. N. (1986). Suppression of prebreakdown current by a cathode coating of CaF_2. *J. Appl. Phys.* 59 (1), p. 283-4. Suppression of prebreakdown current by a cathode coating of silicon. *J. Appl. Phys.* 60 (4), p.1490-2.